Quantum Electronics **52** (3) 227–232 (2022)

https://doi.org/10.1070/QEL18004

Broadband two-dimensional spectrochronography with ultrashort pulses in the mid-infrared

E.A. Stepanov, A.N. Zhdanov, I.V. Savitskii, P.B. Glek,
A.A. Lanin, A.B. Fedotov, A.M. Zheltikov

Abstract. **A novel, 2.6-to-10-μm wavelength-tunable laser source of sub-70-fs pulses is combined with mid-IR heterodyne detection to provide a versatile laser platform for broadband two-dimensional Fourier-transform infrared spectrochronography. The mid-infrared laser output serves as both a short-pulse driver and a broadband probe for time-resolved studies of ultrafast molecular coherence, population dynamics, and multimodal energy transfer in a vast class of complex molecular systems.**

Keywords: *spectrochronography, ultrashort pulses, mid-IR range.*

1. Introduction

The methods of nonlinear optics [1–4] offer unique opportunities for studying fast processes in complex physical, chemical, and biological systems. Multidimensional nonlinear spectroscopy [5–12] is one of the most promising and dynamically developing areas of nonlinear optics. Unlike the methods of conventional, one-dimensional spectroscopy, multidimensional spectroscopy makes it possible to reveal physically and chemically significant classical [7–10] and quantum [11] correlations in the spectra of nonlinear response, as well as to study the dynamics of fast processes in complex atomic and molecular systems [6, 10] and new quantum materials [13].

The methods of 2D Fourier-transform infrared (2D-FTIR) spectroscopy are most widely used to analyse the dynamics of complex organic compounds, in particular, new types of molecular markers used in the analysis of biological complexes [14–19]. Two-dimensional IR spectroscopy makes it possible to obtain information about the environment of proteins reflected in a two-dimensional line shape, to measure the characteristic times of excitation transfer from one vibrational mode to another, to distinguish between solvent-affected and disordered proteins, and to increase the spectral resolution due to the so-called off-diagonal peaks (see Section 5). For example, using 2D-FTIR spectroscopy, new features of the relationship between the vibrational degrees of freedom in nucleic acids were discovered [20–22]. The high temporal resolution of the technique allows analysing the dynamics of peptide folding and protein oligomerisation [21–24], including the technique of labelling cells with the carbon-13 isotope [24].

The use of modern laser systems that generate femtosecond laser pulses in the mid-IR range with a repetition rate up to 100 kHz, as well as fast multi-element linear IR detectors and spatial light modulators to control the pump radiation, allowed the time of recording a two-dimensional spectrum to be reduced to several hundred milliseconds. A significant increase in the signal-to-noise ratio with a decrease in the IR pulse energy by an order of magnitude also became possible [25, 26]. An increase in the rate of recording 2D spectra is also facilitated by the development of algorithms for restoring 2D images from a significantly thinned and shortened data sample, which reduces the minimum number of required readings and increases the signal-to-noise ratio by several times when using *a priori* information about some properties of the recorded signal [27]. Progress in the development of experimental techniques and signal processing methods has made it possible to develop a new promising type of nonlinear optical microscopy based on a two-dimensional IR analysis of coupled vibrational molecular modes [28]. This method assigns some parameters determined from the two-dimensional IR spectrum to each point of the test sample. Thus, in the paper devoted to the observation of protein breakdown in mouse pancreatic tissues [29], the displayed parameters were the fundamental frequency shift of a vibrational mode, the intensity of an off-diagonal peak, and the anharmonicity of vibrational levels, which can only be obtained by applying this technique.

In this paper, we present a universal laser platform for broadband 2D spectroscopy using ultrashort mid-IR pulses. The laser system developed for 2D spectroscopy generates radiation pulses with a duration of less than 70 fs and a wavelength tunable in the range of 2.6–10 μm. Broadband excitation and probing by pulses with such parameters, in combination with the heterodyne detection technique implemented in the mid-IR range, open up possibilities for studying ultrafast dynamics of molecular coherence, as well as ultrafast population kinetics and energy exchange between different degrees of freedom in a wide class of complex molecular systems.

E.A. Stepanov, A.N. Zhdanov, I.V. Savitskii, P.B. Glek, A.A. Lanin, A.B. Fedotov, A.M. Zheltikov Faculty of Physics, Lomonosov Moscow State University, Leninskie Gory 1, stroenie 2, 119991 Moscow, Russia;
e-mail: a.b.fedotov@physics.msu.ru, zheltikov@physics.msu.ru

Received 17 January 2022
Kvantovaya Elektronika **52** (3) 227–232 (2022)
Translated by V.L. Derbov

2. Laser system

Our experiments are based on a laser system (Fig. 1), which is a multifunctional femtosecond Ti:sapphire laser complex, consisting of a master oscillator, a regenerative amplifier, and an optical parametric amplifier [30–32]. The master oscillator generates pulses with a centre wavelength varying in the range of 730–860 nm and a duration of about 30 fs. These pulses are amplified in a regenerative Ti:sapphire amplifier, which produces ~60 fs pulses with an energy of up to 2.4 mJ at a centre wavelength of 790–810 nm. These pulses are used to pump an original two-channel optical parametric amplifier (OPA) that generates tunable radiation at wavelengths of 1100–1550 nm (signal wave) and 1550–2200 nm (idler wave) with pulse energies up to 350 and 200 μJ and durations of about 60 and 55 fs, respectively.

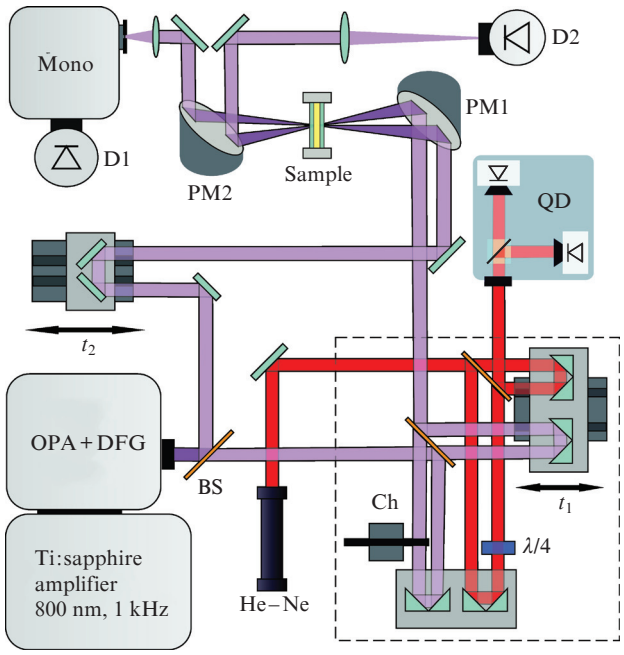

Figure 1. (Colour online) Schematic of a two-dimensional IR spectrometer based on a Michelson interferometer with a quadrature He–Ne detector (QD); (PM1, PM2) off-axis parabolic mirrors; (D1, D2) MCT detectors; (Mono) automated monochromator; (Sample) cuvette with the test substance; (Ch) optical chopper; $\lambda/4$ is the quarter-wave plate.

To generate tunable pulses in the mid-IR region, a 300 μm thick GaSe crystal is used, in which the signal and idler waves are mixed (DFG). By changing the idler and signal wavelengths, it is possible to obtain femtosecond pulses with a duration of 70–100 fs, tunable in the mid-IR range (3–10 μm), which are further divided into replicas and used as pump pulses for 2D-FTIR spectroscopy.

3. Technique of two-dimensional spectroscopy

Nonlinear polarisation arising in a medium under the action of three IR pulses is described by the expression [8]

$$P^{(3)}(t_3,t_2,t_1) \propto \int_0^\infty \mathrm{d}t_3 \int_0^\infty \mathrm{d}t_2 \int_0^\infty \mathrm{d}t_1 R(t_3,t_2,t_1) \times E_3(t-t_3)E_2(t-t_3-t_2)E_2(t-t_3-t_2-t_1), \quad (1)$$

where R is the response function whose measurement is exactly the goal of nonlinear spectroscopy. Different methods of four-wave time-resolved spectroscopy allow determining the response function in various approximations, at zero values of some variables, t_1, t_2 or t_3, or by integrating over them, or by measuring only the modulus of the complex response function. Two-dimensional spectroscopy completely measures the third-order response function using a train of three ultrashort pulses to minimise the effect of convolution on the result. Ideally, when using pulses shorter than the characteristic response times of the system under study, but much longer than the field period, the field strength can be written as

$$E(t) \propto \delta(t)\exp(\pm \mathrm{i}\omega t \mp \mathrm{i}\boldsymbol{k}r \mp \mathrm{i}\varphi), \quad (2)$$

where $\delta(t)$ is a delta function, but the frequency, phase, and wave vector of the field are preserved. In this case, the convolutions in the expression for the nonlinear polarisation disappear, and the generated signal turns out to be directly proportional to the nonlinear response:

$$E^{(3)}_{\mathrm{sig}}(t_3,t_2,t_1) \propto \exp[\mathrm{i}(\mp \boldsymbol{k}_1 \pm \boldsymbol{k}_2 + \boldsymbol{k}_3)\boldsymbol{r}] \times \exp[\mathrm{i}(\mp \varphi_1 \pm \varphi_2 + \varphi_3)]\mathrm{i}R(t_1,t_2,t_3). \quad (3)$$

To determine the amplitude and phase of the response function, heterodyne detection is used, i.e., the measurement of the sum of the nonlinear signal with the local oscillator $E_{\mathrm{loc}}(t-t_{\mathrm{loc}})$, where $t_{\mathrm{loc}} = t_3$, $\boldsymbol{k}_{\mathrm{loc}} = \mp \boldsymbol{k}_1 \pm \boldsymbol{k}_2 + \boldsymbol{k}_3$

$$S(t_1,t_2,t_3) \propto E_{\mathrm{loc}}E^{(3)}_{\mathrm{sig}} \propto \exp[\mathrm{i}(\mp \varphi_1 \pm \varphi_2 + \varphi_3 - \varphi_{\mathrm{loc}})]\mathrm{i}R(t_1,t_2,t_3). \quad (4)$$

Visualisation and interpretation of the third-order response function in the frequency representation turns out to be more intuitively understandable. Therefore, the measured function $S(t_1,t_2,t_3)$ is subjected to a two-dimensional Fourier transform, which is equivalent to the Fourier transform of the third-order response function in the short-pulse approximation (in the case of a precisely phased spectrum, the phase factor is taken to be one):

$$S(\omega_3,t_2,\omega_1) = \int_0^\infty \int_0^\infty S(t_1,t_2,t_3)\exp(\mathrm{i}\omega_1 t_1)\exp(\mathrm{i}\omega_3 t_3)\mathrm{d}t_1\mathrm{d}t_3 = \int_0^\infty \int_0^\infty \mathrm{i}R(t_3,t_2,t_1)\exp(\mathrm{i}\omega_1 t_1)\exp(\mathrm{i}\omega_3 t_3)\mathrm{d}t_1\mathrm{d}t_3, \quad (5)$$

where t_1, t_2 and t_3 are the delays between four IR pulses directly controlled in the experiment. Usually, the Fourier transform is performed over the variables t_1 and t_3, which leads to a set of two-dimensional spectra for various values of the system evolution time t_2, giving complete information about the third-order nonlinear response function $R(\omega_3,t_2,\omega_1)$.

4. Measurement of two-dimensional spectra

In the present work, a two-dimensional IR spectrometer is designed in the pump–probe geometry based on a Michelson interferometer, which forms a pair of pump pulses propagating along one axis with an adjustable delay t_1 [33]. The pump radiation is focused by an off-axis parabolic mirror into the cell with the substance under study together with the third, weak replica of the IR pulse, which plays the role of probe radiation. In this geometry, the nonlinear signal is generated in the same direction as the probe pulse, which, in turn, acts as a local oscillator that amplifies the nonlinear signal. Together they are focused on a monochromator, behind which they are detected by a sensitive mercury–cadmium–tellur (MCT) detector cooled with liquid nitrogen. Since the delay t_3 between the nonlinear signal and the local oscillator (probe pulse) in this geometry turns out to be unchanged, instead of the Fourier transform in this coordinate, radiation is expanded into a spectrum using a monochromator, which immediately gives a signal in the form $S(t_1, t_2, \omega_3)$. To obtain the two-dimensional spectrum $S(\omega_3, t_2, \omega_1)$, it remains to perform a Fourier transform with respect to the variable t_1:

$$S(\omega_3, t_2, \omega_1) = \exp[\mathrm{i}(\varphi_1 - \varphi_2)]$$

$$\times \int_0^\infty S(t_1, t_2, \omega_3) \exp(\mathrm{i}\omega_1 t_1)\, \mathrm{d}t_1. \qquad (6)$$

To maximise the speed of measuring two-dimensional spectra, an automated recording system was assembled, consisting of a synchronous multichannel megahertz ADC (NI USB-6356), two fast radiation detectors in the mid-IR range, two stepper motors for controlling delays t_1 and t_2, a helium-neon quadrature detector, and an optical chopper. To avoid intermediate data interpolation, the Fourier transform is calculated on a nonuniform mesh.

To determine the third-order nonlinear response function in accordance with Eqn. (6), it is necessary to determine very accurately the phase factor, which includes the phase difference of the pump fields $\varphi_1 - \varphi_2$, which is equivalent to finding the absolute delay between the pump pulses. This delay must be measured to a fraction of a period, as otherwise, the mixing of imaginary and real components of the response function in the nonlinear absorption spectrum occurs (the rotation of the vector by $\exp[\mathrm{i}(\varphi_1 - \varphi_2)]$). To phase the spectrum accurately, a femtosecond interferogram of pump pulses is recorded synchronously with the nonlinear signal using the second IR detector (see inset in Fig. 2b), which yields the interferogram spectral phase of the pump transmitted through the sample. The auxiliary detector is installed in the pump beam behind the sample, ensuring a high signal level and an exact match between the phase of the interferogram and the one that acted on the sample, but gives rise to phase distortions near the absorption bands of the sample (green line in Fig. 2b). In the first approximation, however, we can ignore the exact form of the spectral phase of the interference pattern, but restrict ourselves to its linear approximation, which corresponds to a reference frame shift relative to the exact zero delay between two pump pulses, in which all spectral components interfere in phase. Figure 2b shows the linear shift of the spectral phase with an error in choosing the zero delay between pump pulses in one field cycle at a wavelength of 5 μm (16.7 fs).

5. Two-dimensional spectroscopy of complex molecular systems

The 2D-FTIR spectrometer described was used to measure the two-dimensional IR correlation spectrum of the cobalt

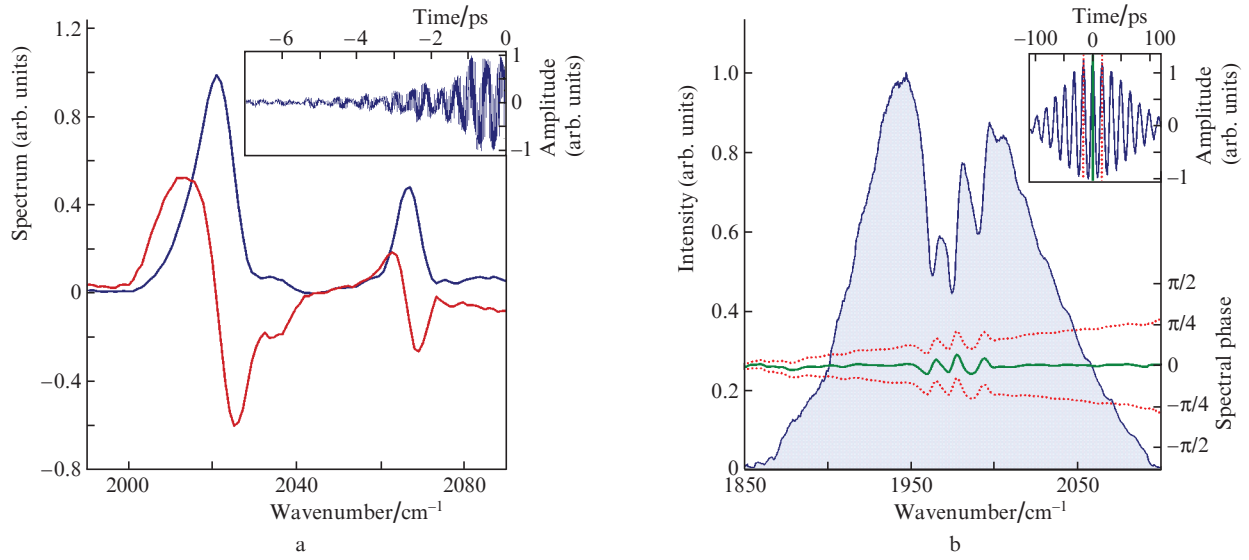

Figure 2. (Colour online) Exact phasing of the two-dimensional spectrum in terms of the spectral phase of the autocorrelation function: (a) the real (blue curve) and imaginary (red curve) components of the Fourier spectrum of the substance nonlinear response (the signal is shown in the inset); (b) Fourier spectrum (filled blue curve) and spectral phase (green curve) of the autocorrelation function of the pump pulses (shown in the inset) measured behind the sample with detector D2, the pointed line shows the spectral phase at the zero delay between pulse per radiation period at the central wavelength 5 μm (~16.5 fs).

carbonyl complex of composition $Co_2(CO)_8$ in hexane solution. Metal carbonyls are used as reagents and catalysts and have important practical applications in organometallic chemistry and organic synthesis. The substance under study has pronounced absorption lines near 2000 cm^{-1} (about 5 μm) in the set of frequencies corresponding to different CO vibrational modes. In an alkane solution, dicobalt octacarbonyl exists in three stable states corresponding to different isomers [34], giving rise to off-diagonal peaks – a nonlinear signal corresponding to the response of the studied molecule at a frequency different from the excitation frequency, which lies off the $\omega_{pump} = \omega_{probe}$ diagonal of the two-dimensional map and, therefore, bears information about both the redistribution of energy within one isomer and the change in the state of the molecule and its transition from one isomer to another after exciting the vibration by a femtosecond laser pulse.

The studied substance in the liquid state is placed in a 100 μm thick cuvette with calcium fluoride windows. In the experiments performed, a solution of cobalt carbonyl in hexane with an initial concentration of 50 μg mL^{-1} was diluted with a solvent to reduce the optical density at wavelengths corresponding to the highest absorption in the region of 2000 cm^{-1} to a value of about one. In the used pump–probe beam geometry, the probe pulse itself acts as a local oscillator, since it propagates strictly in the same direction as the nonlinear signal [33]. The resolution of the excitation spectrum is determined by the sample length of scanning the variable t_1. Thus, to obtain a resolution of ~1 cm^{-1} (which corresponds to 100 points in the wave number range of interest to us, 1990–2090 cm^{-1}, where the absorption lines of vibrational modes of all cobalt carbonyl isomers are located), it is necessary to scan the delay in the range of 30 ps. The second automated translation stage with a retroreflector is used to control with femtosecond accuracy the delay t_2 between a pair of pump pulses and a probe pulse. Measurement of two-dimensional spectra at different values of the parameter t_2 allows one to trace the vibrational dynamics of a molecular complex with a resolution of a few femtoseconds.

The results presented in Fig. 3a clearly demonstrate that even a single two-dimensional spectrum of the substance under study allows a distinct identification of the overlapping absorption spectra of several different isomers, which fundamentally cannot be separated chemically, since they interconvert into each other on a picosecond time scale. Thus, the absorption lines of isomers I and II near 2070 cm^{-1}, indistinguishable in the one-dimensional Fourier spectrum (black curve in Fig. 3c), exhibit substantially different cross-peak patterns in the 2D image, which allow not only separating them from each other, but also correlating with other eigenfrequencies of each isomer. The line having a higher frequency, ~2073 cm^{-1}, forms two pronounced off-diagonal peaks with a central absorption line with a wavenumber of ~2045 cm^{-1}; in the two-dimensional spectrum, these off-diagonal peaks have coordinates of 2045, 2073 cm^{-1} and 2073, 2045 cm^{-1}. At the same time, the line at ~2065 cm^{-1} forms pronounced peaks with coordinates 2020, 2065 cm^{-1} and 2065, 2020 cm^{-1}. This testifies in favour of the fact that the lines at 2020 and 2065 cm^{-1} are inherent in one isomer, and the lines at 2045 and 2073 cm^{-1} in another, which coincides with the results of the experiment and numerical simulation performed in Ref. [34].

However, much more information about the structure and vibrational dynamics of the compound can be provided by the time dependence of the two-dimensional spectra on the

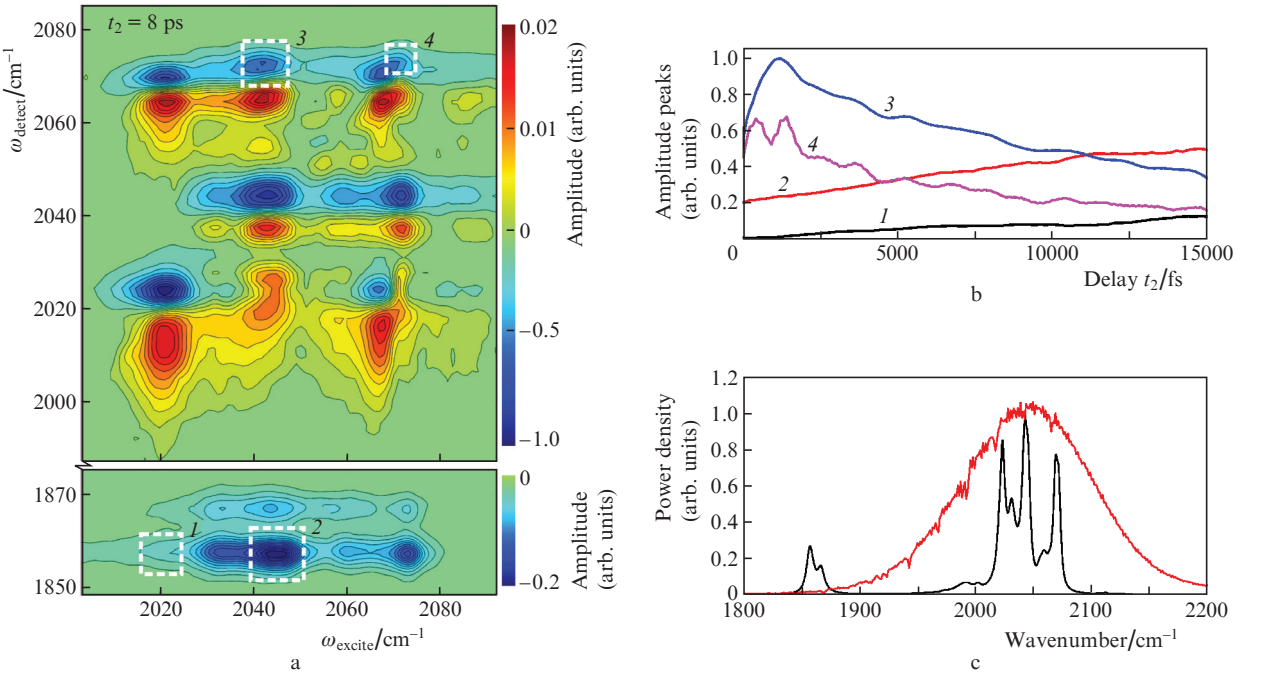

Figure 3. (Colour online) (a) Two-dimensional IR spectrum of dicobalt octacarbonyl measured for a delay t_2 = 8 ps; (b) dependences of the amplitudes of peaks *1*–*4* (framed by dashed squares in the panel in Fig. a) on the delay t_2 in the range of 0–15000 fs; (c) Fourier absorption spectrum of octacarbonyldicobalt (black curve) and IR spectrum of pump/probe radiation (red curve).

delay between the pump pulses and the probe pulse. By varying the duration of the so-called 'evolution time' of a molecular system, one can observe the redistribution of energy between different vibration modes with a femtosecond resolution. To demonstrate this possibility, we measured the time dependences of the excitation spectra for several detection frequencies in our experiments. Figure 3b shows a two-dimensional image of the excitation spectrum versus time t_2 scanned in the range of 0–15 ps with a step of 100 fs for a detection frequency of 2073 cm^{-1}. The normalised intensities of the diagonal peak at a pump frequency of 2073 cm^{-1} [curve (*4*)] and the off-diagonal peak at a pump frequency of 2045 cm^{-1} curve (*1*)], calculated as integrals of the excitation spectrum in the vicinity of the lines, are shown (with the opposite sign for convenience of perception) in Fig. 3b. The dependences demonstrate damped periodic oscillations against the background of an exponential decay. Regular fluctuations in the intensity of the peaks are associated with the energy transfer between vibrational modes. A correlation analysis of the time dependences of the intensities of all observed diagonal and off-diagonal peaks makes it possible to reveal the direction and rate of reactions, to refine the energy parameters of states, and to identify the influence of the environment of a molecule on its vibrational dynamics [34]. However, in our experiments with a single-element detector, we were only able to measure time dependences for three distinct detection wavelengths.

As a result of using tunable broadband femtosecond pulses and a registration system with low-noise MCT detectors cooled by liquid nitrogen, our system allowed us to measure the correlation of vibrational lines not only near 2000 cm^{-1}, where the pump spectral density is maximum, but also in the region 1850–1870 cm^{-1} using the long-wavelength IR spectrum wing (red curve in Fig. 3c). Both detected lines at frequencies of 1857 and 1866 cm^{-1} are responsible for vibrations of the bridging CO ligand, which is present only in isomer I [35]. This result is confirmed by our two-dimensional spectra in this region: the brightest off-diagonal peaks corresponding to the pumping of isomer I (including peak *2* at a pump frequency near 2045 cm^{-1}, Fig. 3a), are present at zero delays t_2, gradually increasing with its increase [curve (*2*) in Fig. 3b], whereas the other peaks corresponding to pumping isomers II and III (including peak *1* at the pump frequency near 2020 cm^{-1} in Fig. 3a) are absent at zero delay, but also appear and grow with its increase [curve (*1*) in Fig. 3b]. From the measured time dependences, one can determine the relaxation rate of excitation from higher-frequency modes of isomer I to lower-energy modes, and also see the rate at which the transformation of the first isomer into the second and third occurs.

6. Conclusion

Thus, we have presented a universal laser platform for broadband spectroscopy based on the use of ultrashort mid-IR pulses. The laser system developed for 2D spectroscopy generates radiation pulses with a duration of less than 70 fs and a wavelength tunable in the range of 2.6–10 μm. Broadband excitation and probing performed by pulses with such parameters, in combination with the heterodyne detection technique implemented in the mid-IR range, provide important advantages over the methods of one-dimensional nonlinear optical spectroscopy [36, 37], opening up possibilities for studying the ultrafast dynamics of molecular coherence, as well as ultrafast population kinetics and energy exchange between different degrees of freedom in a wide class of complex molecular systems.

Acknowledgements. This work was supported by the Russian Foundation for Basic Research (Grant Nos 18-02-40025 and 19-29-12062).

References

1. Akhmanov S.A., Khokhlov R.V. *Problemy nelineinoi optiki* (Problems of Nonlinear Optics) (Moscow: VINITI, 1964).
2. Bloembergen N. *Nonlinear Optics* (New York: Benjamin, 1965).
3. Akhmanov S.A., Koroteev N.I. *Metody nelineinoi optiki v spektroskopii rasseyaniya sveta* (Methods of Nonlinear Optics in Light Scattering Spectroscopy) (Moscow: Nauka, 1981).
4. Mukamel S. *Principles of Nonlinear Optical Spectroscopy* (New York: Oxford University Press, 1995).
5. Asplund M.C., Zanni M.T., Hochstrasser R.M. *Proc. Nat. Acad. Sci.*, **97** (15), 8219 (2000).
6. Hamm P., Lim M., Hochstrasser R.M. *J. Phys. Chem. B*, **102** (31) 6123 (1998).
7. Mukamel S., Tanimura Y., Hamm P. *Acc. Chem. Res.*, **42** (9), 1207 (2009).
8. Hamm P., Zanni M. *Concepts and Methods of 2D Infrared Spectroscopy* (Cambridge: Cambridge University Press, 2011).
9. Cundiff S.T., Mukamel S. *Phys. Today*, **66**, 44 (2013).
10. Dai X., Bristow A.D., Karaiskaj D., Cundiff S.T. *Phys. Rev. A*, **82**, 052503 (2010).
11. Dorfman K.E., Schlawin F., Mukamel S. *Rev. Mod. Phys.*, **88**, 045008 (2016).
12. Koroteev N.I. *Vestn. Mosk. Univ., Ser. 3: Fiz. Astron.*, (6), 6 (1996).
13. Smallwood C.L., Ulbricht R., Day M.W., Schröder T., Bates K.M., Autry T.M., Diederich G., Bielejec E., Siemens M.E., Cundiff S.T. *Phys. Rev. Lett.*, **126**, 213601 (2021).
14. Park K.-H., Choi S.R., Choi J.-H., Park S., Cho M. *Chem. Phys. Chem.*, **11**, 3632 (2010).
15. Brookes J.F., Slenkamp K.M., Lynch M.S., Khalil M. *J. Phys. Chem. A*, **117**, 6234 (2013).
16. Simpson N., Shaw D.J., Frederix P.W., Gillies A.H., Adamczyk K., Greetham G.M., Towrie M., Parker A.W., Hoskisson P.A., Hunt N.T. *J. Phys. Chem. B*, **117**, 16468 (2013).
17. Dutta S., Li Y.-L., Rock W., Houtman J.C.D., Kohen A., Cheatum C.M. *J. Phys. Chem. B*, **116**, 542 (2012).
18. Tucker M.J., Gai X.S., Fenlon E.E., Brewer S.H., Hochstrasser R.M. *Phys. Chem. Chem. Phys.*, **13**, 2237 (2011).
19. Kim H., Cho M. *Chem. Rev.*, **113**, 5817 (2013).
20. Tucker M.J., Abdo M., Courter J.R., Chen J., Brown S.P., Smith A.B., Hochstrasser R.M. *Proc. Nat. Acad. Sci.*, **110**, 17314 (2013).
21. Ganim Z., Jones K.C., Tokmakoff A. *Phys. Chem. Chem. Phys.*, **12**, 3579 (2010).
22. Maekawa H., De Poli M., Toniolo C., Ge N.-H. *J. Am. Chem. Soc.*, **131**, 2042 (2009).
23. Jones K.C., Peng C.S., Tokmakoff A. *Proc. Nat. Acad. Sci.*, **110**, 2828 (2013).
24. Moran S.D., Zhang T.O., Zanni M.T. *Protein Sci.*, **23**, 321 (2014).
25. Farrell K.M., Ostrander J.S., Jones A.C., Yakami B.R., Dicke S.S., Middleton C.T., Hamm P., Zanni M.T. *Opt. Express*, **28** (22), 33584 (2020).
26. Donaldson P.M., Greetham G.M., Shaw D.J., Parker A.W., Towrie M. *Phys. Chem. A*, **122** (3), 780 (2018).
27. Humston J.J., Bhattacharya I., Jacob M., Cheatum C.M. *J. Chem. Phys.*, **150**, 234202 (2019).
28. Ostrander J.S., Serrano A.L., Ghosh A., Zanni M.T. *ACS Photonics*, **3** (7), 1315 (2016).

29. Dicke S.S., Alperstein A.M., Schueler K.L., Stapleton D.S., Simonett S.P., Fields C.R., Chalyavi F., Keller M.P., Attie A.D., Zanni M.T. *J. Phys. Chem. B*, **125**, 9517 (2021).
30. Lanin A.A., Stepanov E.A., Fedotov A.B., Zheltikov A.M. *Optica*, **4**, 516 (2017).
31. Stepanov E.A., Lanin A.A., Voronin A.A., Fedotov A.B., Zheltikov A.M. *Phys. Rev. Lett*., **117**, 043901 (2016).
32. Lanin A.A., Voronin A.A., Stepanov E.A., Fedotov A.B., Zheltikov A.M. *Opt. Lett*., **40,** 974 (2015).
33. Helbing J., Hamm P. *J. Opt. Soc. Am. B*, **28** (1), 171 (2011).
34. Anna J.M., Kubarycha K.J. *J. Chem. Phys*., **133**, 174506 (2010).
35. Sweany R.L., Brown T.L. *Inorg. Chem*., **16** (2), 415 (1977).
36. Zheltikov A.M., Koroteev N.I. *Phys. Usp*., **42**, 321 (1999) [*Usp. Fiz. Nauk*, **169** (4), 385 (1999)].
37. Zheltikov A.M. *J. Raman Spectrosc*., **31**, 653 (2000).